Chapter 3

PCDTBT:PCBM:CdSe Tetrapod Shaped Nanocrystals Hybrid Nanocomposites Based UV-Visible Photodetectors

Content of this Chapter

Part of this work has been published as:

- **D. C. Upadhyay** et al., "PCDTBT: PCBM: CdSe Tetrapod Shaped Nanocrystals Hybrid Nanocomposites based UV-Visible Photodetectors," in ***IEEE Photonics Technology Letters***, doi: 10.1109/LPT.2021.3088219. (IF: **2.451)**

Chapter 3

PCDTBT: PCBM:CdSe Tetrapod Shaped Nanocrystals Hybrid Nanocomposites based UV-Visible Photodetectors

3.1 Introduction

The UV-Visible (Vis) broadband photodetectors find exciting and potential applications in biomedical imaging, ultra-violet astronomy and wide spectral switches[33], [102]. In general, most of the inorganic-organic hybrid nanocomposite-based UV-Visible photodetectors use spherical shaped inorganic NCs as a sensitizer to enhance the detection spectral range of the device[103]. In such nanocomposites, the inorganic NCs act as a sensitizer while polymer composites serve as functional interfaces to extract charge carriers from the inorganic sensitizer [104]. However, the composite polymers may also allow ambipolar transport in the ternary blend nanocomposite-based devices [79]. In order to avoid it, few researchers have explored branched structures (e.g. tetrapod shaped) of inorganic NCs in place of the conventionally used nanorods and spherical quantum dots shaped NCs in ternary nanocomposites for fabricating high performance solar cells [105], [106]. It is shown that the tetrapod shaped CdSe NCs material possesses ultrafast carrier dynamics in the fabricated solar cells [107]. It is further reported that the electron transfer is independent of the orientations of NCs in the tetrapod shaped CdSe NCs based solar cells which favors ultrafast separation of electrons from NCs to organic electron acceptors [107].

Based on the above observations, the present chapter is devoted to investigate the performance characteristics of FTO/ZnO NRs/PCDTBT: PCBM:CdSe NCs/MoOx/Ag based UV-Visible photodetector where PCDTBT stands for Poly[N-9″-heptadecanyl-2,7-carbazole-

alt-5,5-(4′,7′-di-2-thienyl-2′,1′,3′benzo-thiadiazole)] polymer and PCBM represents the [6, 6]-phenyl C_{61} butyric acid methyl ester. In this new ternary nanocomposite, the tetrapod shaped CdSe NCs are mixed with the PCDTBT: PCBM binary nanocomposite to achieve a wide absorption spectrum of the active material covering the UV-Visible region. The ZnO NRs layer acts as a UV absorber as well as an efficient ETL in the proposed structure[108]. The active layer of PCDTBT: PCBM:CdSe NCs nanocomposite is deposited over the ZnO NRs so that the NRs can penetrate into the active layer to improve the performance of proposed photodetector by reducing the dark current as discussed in Chapter-2. The thin MoOx layer is used as the hole transport layer (HTL) as considered in Chapter 2. The MoOx layer was deliberately used to reduce the degradation of the device by providing a barrier to oxygen and preventing unnecessary diffusion of metal ions inside the active layer[109].

3.2 Experimental Methodology

3.2.1 Materials Used and Synthesis

All chemicals and materials used for the device fabrication process have been procured from Sigma–Aldrich/Merck Chemicals and they have been used directly without any further purification. The CdSe tetrapod shaped NCs have been synthesized by following similar steps described in [110] with some slight modifications. Selenium stock solution was prepared by mixing 30mg of selenium, 5 mL of 1 octadecene and 0.4 mL of trioctylphosphine in a 10 mL round bottom flask. The cadmium precursor was prepared by adding 13 mg of CdO, 0.6 mL of oleic acid and 10 mL of octadecene in a 25 mL round bottom flask. The cadmium precursor solution was slowly heated and when it reached 225 °C, 1 mL of the selenium solution was quickly injected into it and then waited for 60 seconds. Once the solution takes a light orange colour, the solution was centrifuged and was

then washed three times with ethanol to obtain CdSe NCs. Solution of PCDTBT: PCBM: CdSe tetrapod nanocomposites were then prepared by mixing them with weight ratios of (1:4:1, wt. /wt. /wt.) for fabricating active layer of the device. PCDTBT is dissolved in 1, 2 – dichlorobenzene while PCBM and CdSe NCs were separately dissolved in chloroform. These separate solutions were kept under continuous stirring for more than 20 hours before mixing to get the desired nanocomposites. The prepared nanocomposites were again kept under continuous stirring for 1 hour before final use.

3.2.2 Device Fabrication

Fluorine-doped tin oxide (FTO)-coated glass substrates were subsequently washed ultrasonically for 5 min by soap solution, deionized water (DI water), and acetone. ZnO nanorods based ETL was then grown on the cleaned FTO substrates by following the method described in our earlier work with slight modification[111].In this method, a seed layer ZnO QDs (prepared by the method reported in[112]) of ~ 50 nm thickness was fabricated on the cleaned FTO substrate by the spin coating method. The seed layer was then annealed at 150^0C for 15 minutes. Finally, the seed layer coated substrate was kept in the solution of 0.01M zinc nitrate dehydrate and 0.01M hexamethylenetetramine at 85^0C for 120 minutes. The samples were then washed rigorously with DI water and then they were annealed at 400 ^{0}C in an open environment to get the desired ZnO nanorods based ETL of the device. The hydrothermal synthesis of ZnO NRs preparation is pictorially represented with the help of Fig.3.1 as shown below.

The active layer was obtained by spin coating of PCDTBT: PCBM: CdSe tetrapod nano-composite solution on the ETL. The coated active layer was annealed at 120 ^{0}C in an open

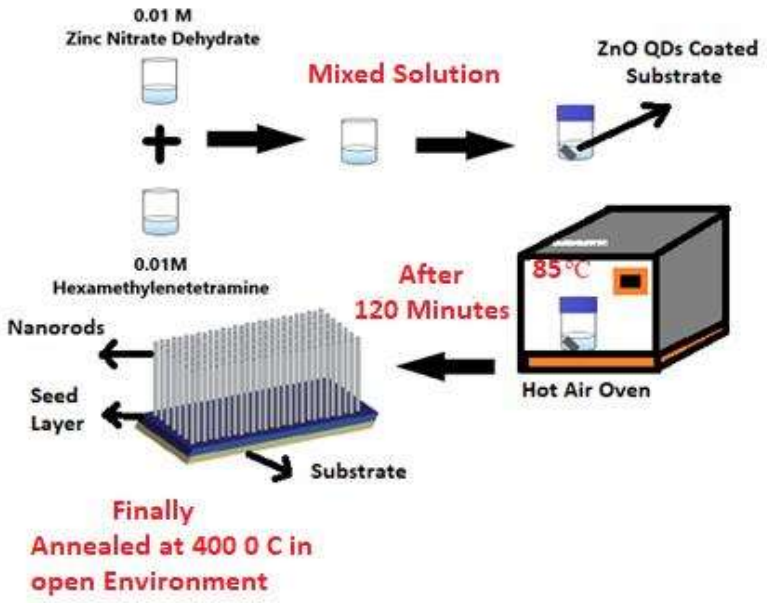

Fig. 3.1 Represents the schematic of Hydrothermal synthesis of ZnO nanorods.

environment. A thin MoOx layer of thickness ~ 10 nm was deposited on the active layer by thermal evaporation method.Silver (Ag) electrode was deposited on the HTL in the form of metal dots with an effective area of 0.0314 $cm^2$and of ~120 nm thickness by following the same thermal evaporation method [112]. The schematic of the proposed device structure and its corresponding energy band diagram are shown in Fig.3.2 (a) and (b) respectively.

3.3 Results and Discussion

3.3.1 Material Characterization

The TEM image of the as synthesized CdSe NCs is shown in Fig. 3.3 (a) and Fig. 3.2 (b), to confirm the tetrapod shapes of the NCs. The corresponding vertically well-aligned ZnO nanorods high-resolution SEM (HRSEM) image is depicted in the Fig.3.4 (a),(b). The typical hexagonal cross-section is evident from the HRSEM image of penetrated electron transport layer as grown on the FTO substrate.

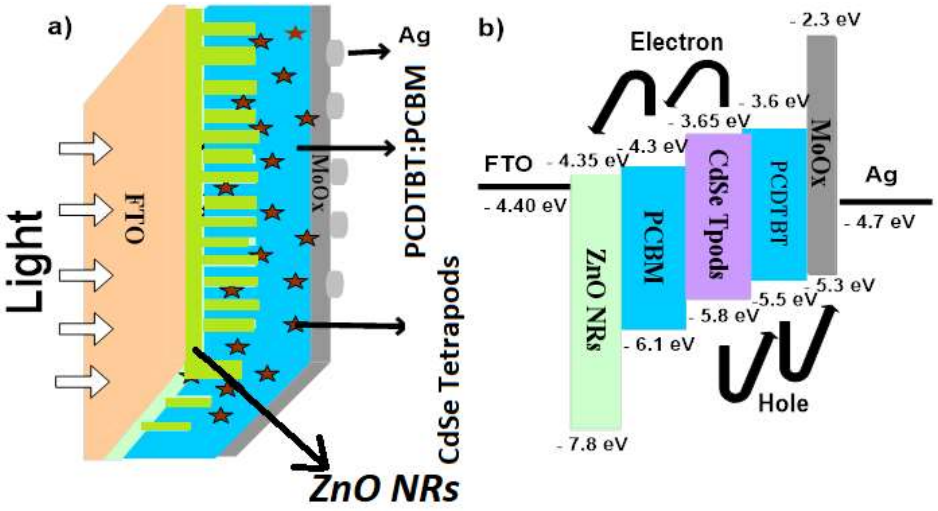

Fig.3.2. (a). Schematic of inverted device structure (b) Flat energy band diagram of the proposed device

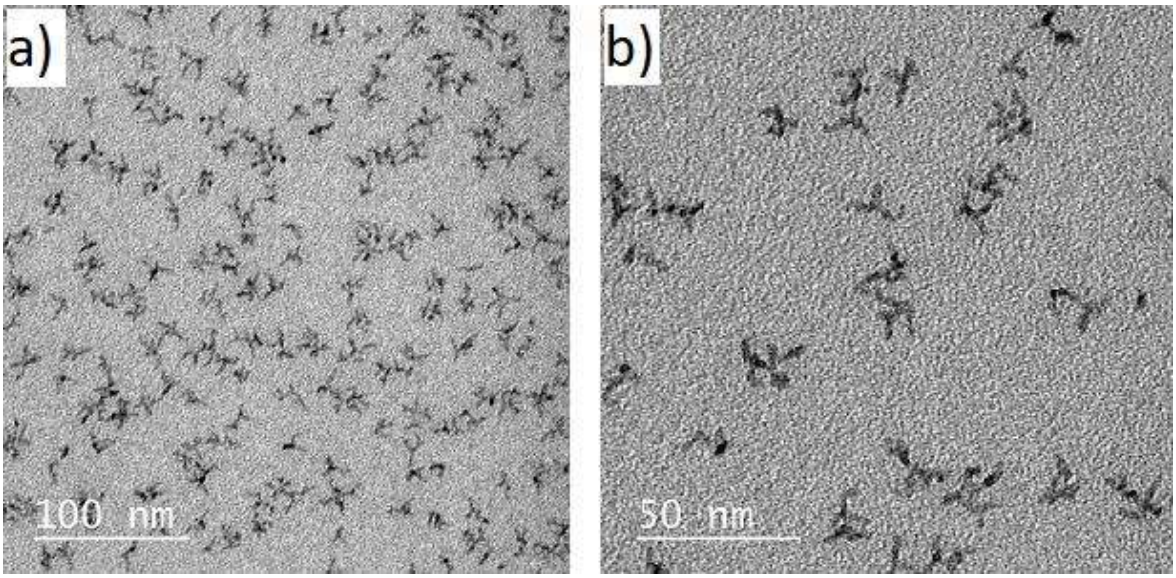

Fig.3.3: Typical TEM micrograph of CdSe NCs (a) 100 nm and (b) 50 nm scale

It is well known that proper band alignment is necessary for achieving the high performance of a photodetector device[91]. Step like energy band alignment is necessary requirement to assist smooth and efficient charge transfer in the device[92]

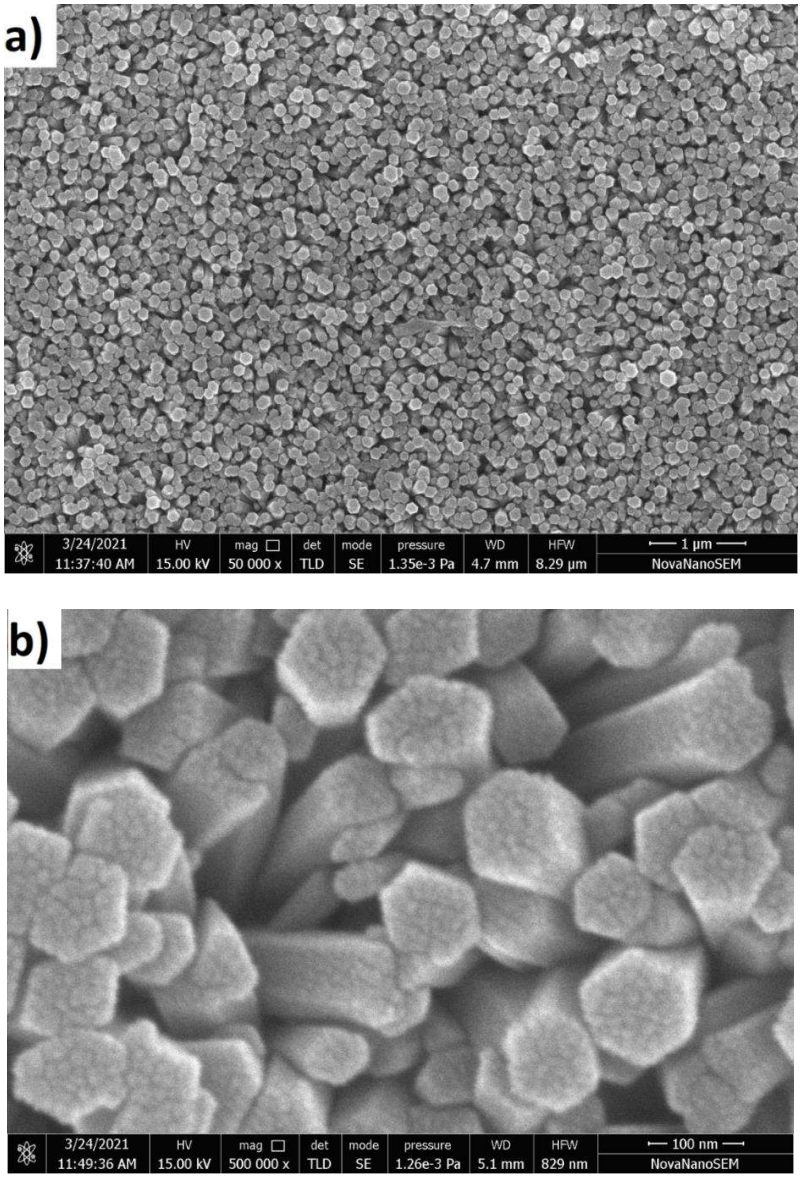

Fig.3.4: HRSEM image of as-grown ZnO nanorods on FTO substrate (a)1 - µm scale (b) 100 nm scale.

It can be visualized from the energy band diagram of our proposed photodetectors as depicted in the Fig.3.2 (b).Fig.3.5 compares the absorption characteristics of the tetrapod shaped CdSe nano-crystals, PCDTBT:PCBM and PCDTBT: PCBM: CdSe tetrapod shaped nano-composites. The absorption spectrum of the CdSe tetrapod covers both the UV and visible regions up to ~600 nm with a small peak at ~ 540 nm. The absorption of

PCDTBT:PCBM blends also cover both UV and visible regions with a peak at ~ 550 nm. The absorption curve PCDTBT: PCBM: CdSe and PCDTBT:PCBM clearly shows an overall increase in the absorption in the UV and visible bands as compared to their respective absorptions of the CdSe NCs and PCDTBT: PCBM layer. It may be observed that the absorption peaks of CdSe: PCDTBT:PCBM nanocomposites are higher than those of PCDTBT: PCBM blends but are close to those of the PCDTBT:PCBM blends. Because the concentration of CdSe NCs in the nanocomposite is very small as compared to that in the CdSe NCs films used for absorption measurements.

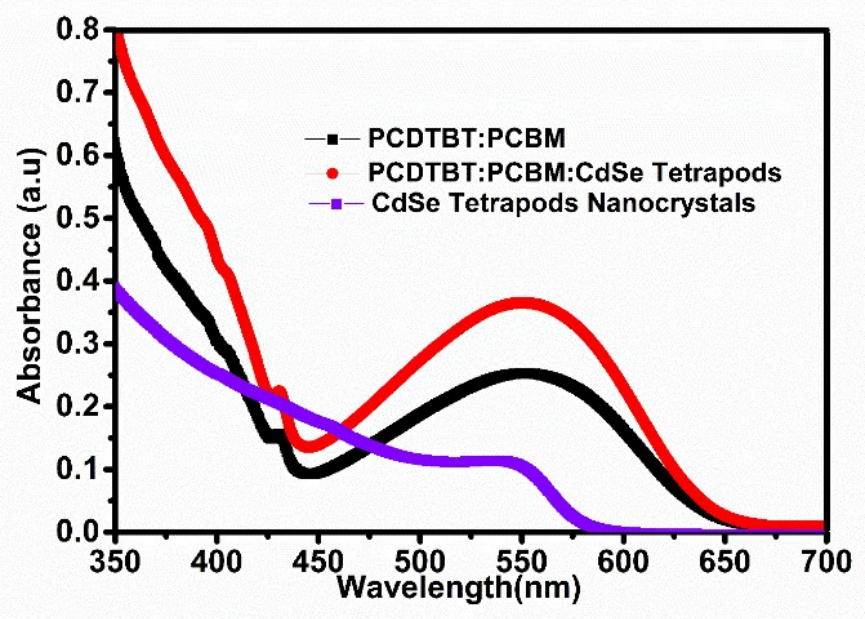

Fig.3.5 UV-Visible absorption plot of tetrapod shaped CdSe nano-crystals, PCDTBT: PCBM and PCDTBT: PCBM: CdSe Tetra pod nano-composites respectively

3.3.2 Electrical and Optical Characterization

The electrical performance of the device under dark and illumination conditions were measured in an open-air environment using a parameter analyzer (Key sight: Model B1500A).

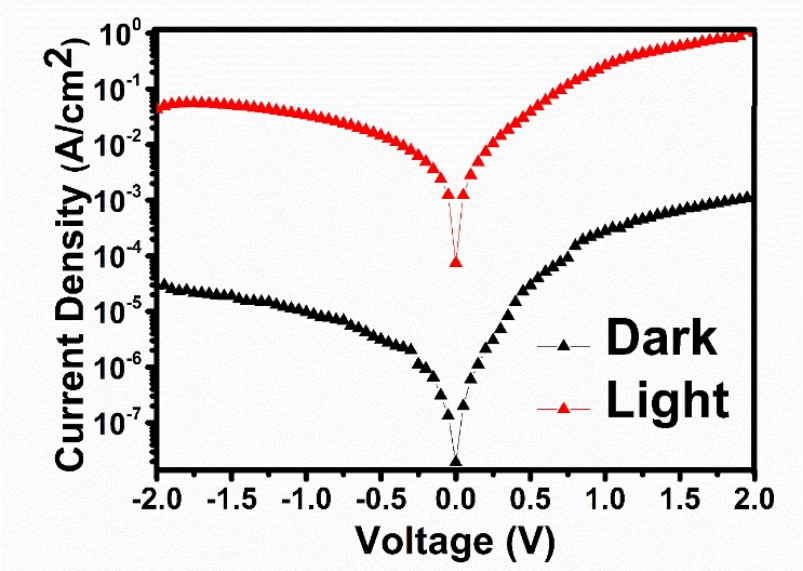

Fig. 3.6 : Logarithmic Current Density -Voltage (J-V) plot under dark and illumination condition of a broadband light source of intensity 100 mW/cm^2.

Current Density (J)-Voltage (V) characteristics of the fabricated device under dark and broadband light of intensity 100mW/cm^2 illumination are compared in Fig.3.6. The significant photocurrent is observed under reverse bias operation.

High current levels under forward and reverse bias conditions shown in Fig.3.6 confirms proper charge injection within the device[113]. The analysis of J-V characteristics shows the presence of a small photovoltaic effect with an open circuit voltage of ~1.8 mV which may be attributed to the wide absorption spectra of PCDTBT: PCBM: CdSe tetrapod layer . . Fig.3.7 (a), (b) and (c) demonstrates the photoresponse behavior of the proposed photodetector under modulated lights (repeated on/off) in broadband, UV and visible regions. Interestingly, no change in the photoresponse patterns were observed under the illumination of modulated lights. These unchanged photoresponse characteristics confirm the high stability of our proposed organic-inorganic hybrid photodetector device under open atmospheric

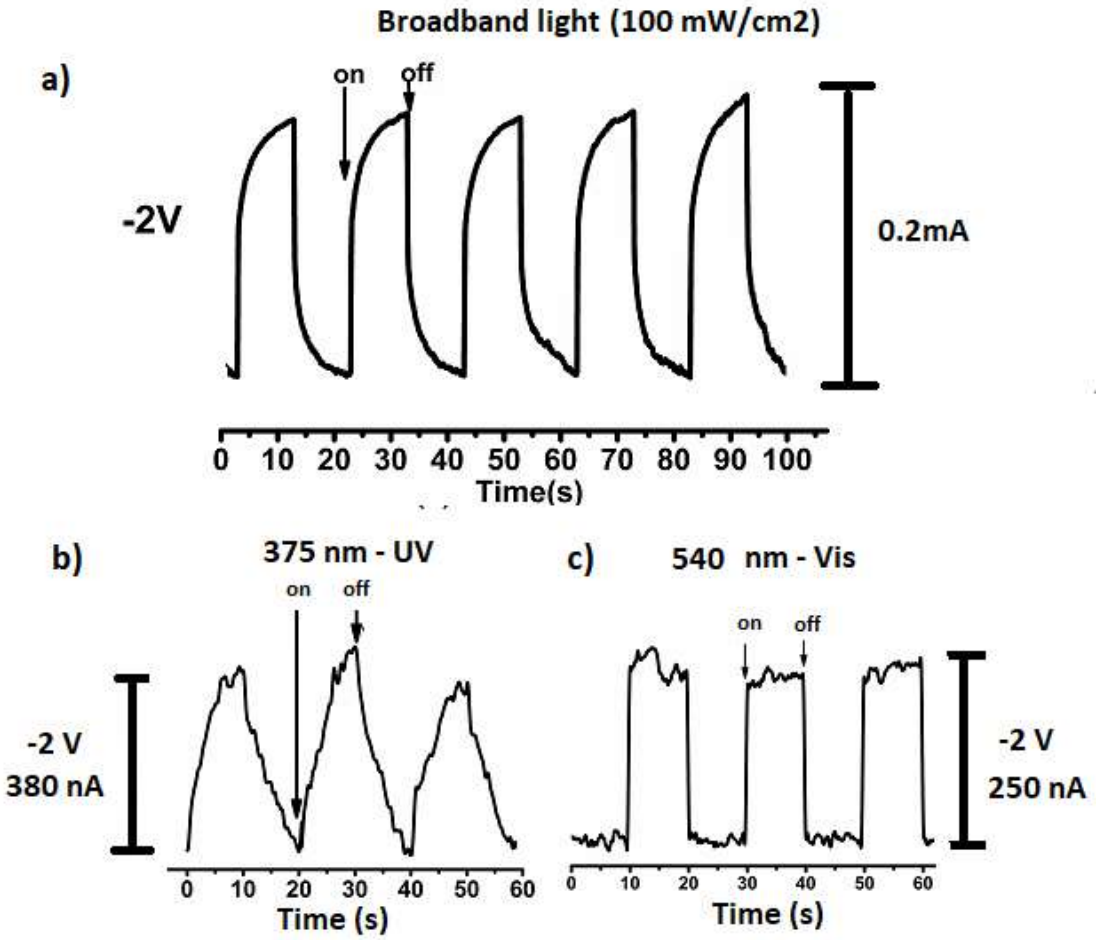

Fig.3.7: .Photoresponse plot of the device under light modulation (on/off) (a) multiple cycles of photoresponse under broadband light intensity with power density (P_d) of 100 $mWcm^{-2}$ (b) UV-375 nm with P_d of 13.1μWcm^{-2} and (c) Visible-540 nm light with P_d of 41.2μWcm^{-2}respectively

condition[113].Further,Fig.3.7 (c) reveals that the response speed of our proposed device to visible light is faster than broadband and UV light.

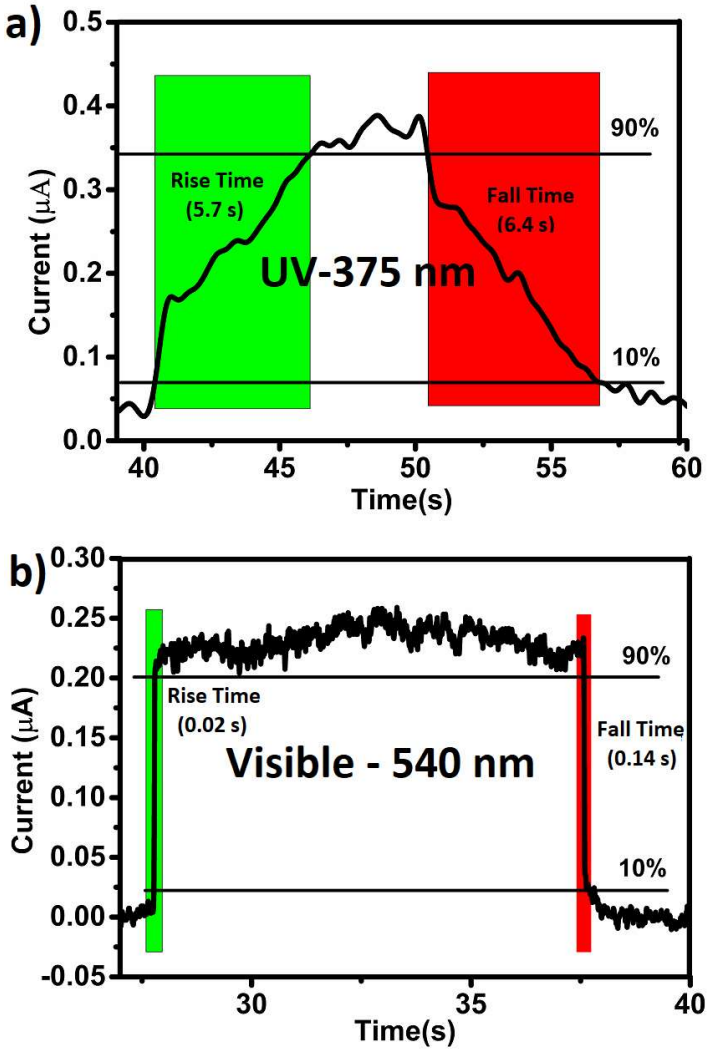

Fig.3.8: .Response time calculation of the device illuminated with (a) wavelength 375 nm (UV) under P_d of 13.1 μWcm^{-2}(b) wavelength 540 nm (Vis) under P_d of 41.2 μWcm^{-2}

The rise time (τ_{rise}) and fall time (τ_{fall}) were examined in Fig.3.8. The measured rise time of τ_{rise}~0.02s (τ_{rise}~5.73s) and fall time of τ_{fall}~ 0.14s (τ_{fall}~ 6.41s) were obtained under visible (UV)light illumination.The superior response speed under visible light is attributed to ultra-fast charge separation from tetrapod to the organic electron acceptor layer and further by employing the penetrated ZnO nanorods based ETL[108].

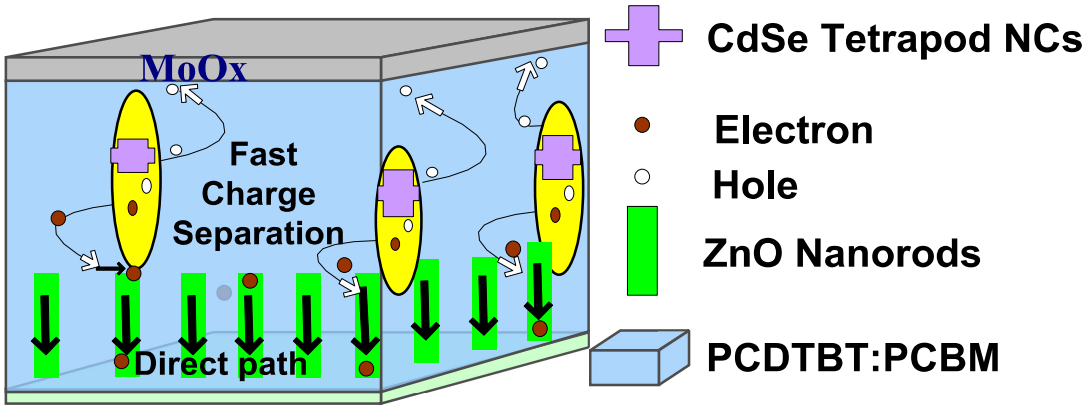

Fig.3.9. Pictorial illustration of the mechanism in the proposed device under excitation of visible light.

The proposed mechanism for the superior response speed of the device under visible light is elucidated with the help of the charge transfer mechanism as shown in Fig.3.9. Herein, CdSe tetrapod NCs basically act as an electron donor and PCBM work as an electron acceptor. It may also mention that the proposed device is fabricated in an open environment condition. This may lead to some defects which, in turn, may reduce the response speed of the device [114]. Thus, fabrication in a controlled

environment is expected to improve the speed of our device. Further, low mobility and the large resistance-capacitance time constant of polymer-based devices, in general, results in low response speed [114]. However, the measured rise-time and fall-time in both the UV and visible regions of our proposed device fabricated under an open environmental condition are much better than several ZnO nanostructure-based UV-Visible photodetectors reported in the literature [115].

The CdSe tetrapod NCs exhibit fast separation of electrons from the tetrapod to organic acceptors which are finally reached to the respective electrode via ZnO nanorods based ETL. Electrons separated from the tetrapod may get diffused through PCBM but the employment

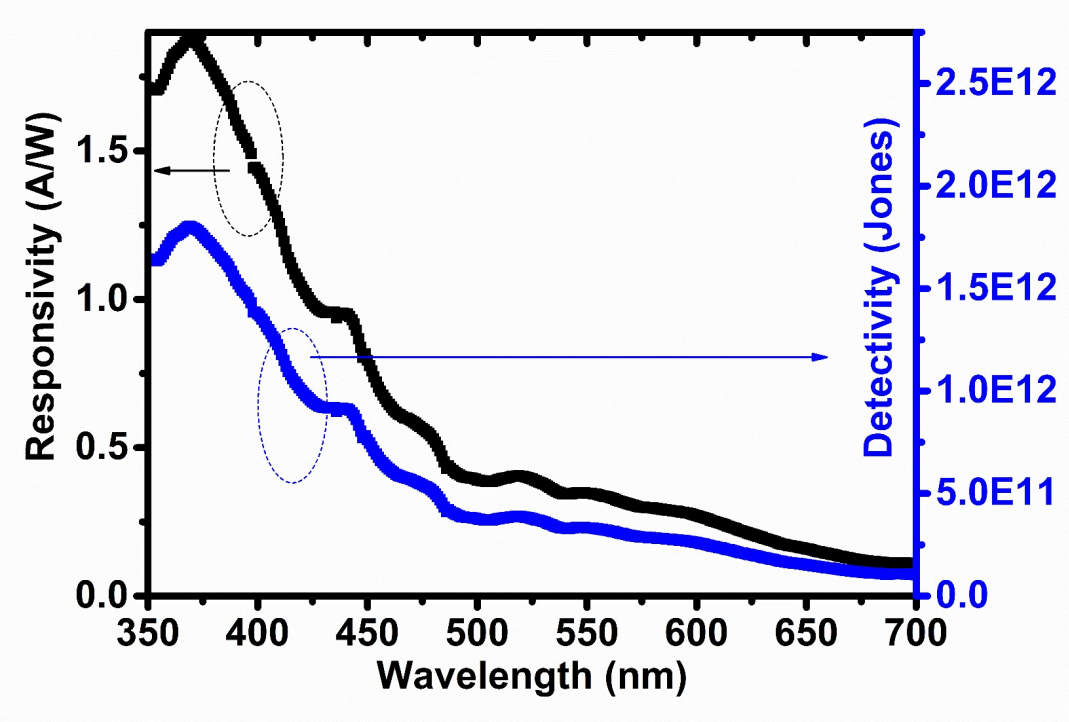

Fig.3.10: Responsivity (R_λ) and Detectivity (D) plot as a function of over a spectral range from 350 to 700 nm.

of nanostructures like ZnO nanorods penetrated well within the active layer further assist the direct collection of ultrafast separated charge carrier generated throughout the device as reported previously[112].

Finally, more optical characterizations of the device were performed by using a monochromator (SP2150i from Princeton Instruments, USA) under the open environmental condition to gain more insight into the performance of our proposed device. Fig.3.10 shows the responsivity and detectivity characteristics plotted as a function of Wavelength over spectral range from 350 to 700 nm.

The responsivity (R_λ) and detectivity (D) were calculated by using the following equations[112].

$$R_\lambda(A/W) = \frac{I_{ph}}{P_{in}}, \quad (3.1)$$

$$D(Jones) = \frac{R_\lambda}{\sqrt{2eJ_d}} \quad (3.2)$$

Where, R_λ is the responsivity in (A/W) and λ is wavelength in (nm), I_{Ph} is the measured photocurrent, J_d is the dark current density (A/cm2) and e (C) is the electron charge and P_{IN} is the incident optical power on the device.

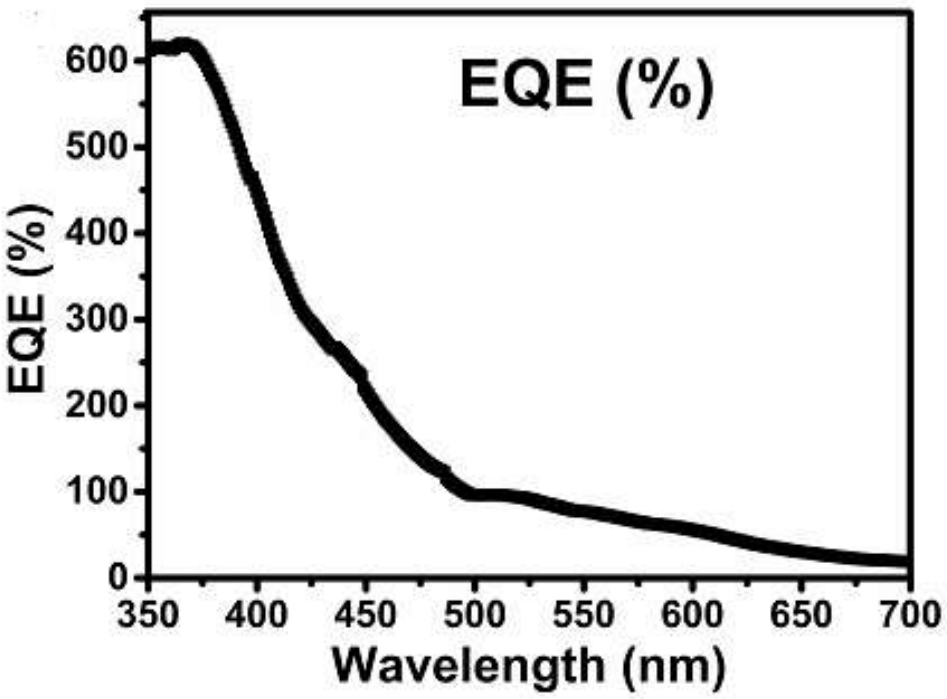

Fig.3.11: EQE plot as a function of over a spectral range from 350 to 700 nm.

The EQE (%) plot as a function of wavelength over a spectral range from 350 nm to 700 nm is also shown in the Fig.3.11. The EQE is determined from the following equations [112].

$$EQE(\%) = 1240\frac{R_\lambda}{\lambda} * 100 \qquad (3.3)$$

Where, R_λ is the responsivity in (A/W) and λ is wavelength in (nm).

The measured values of the responsivity, detectivity and EQE by using above equation are found to be 1830 mA/W(~344 mA/W),~$1.75x10^{12}$(~$3.3x10^{11}$) Jones and 603.19 %(81.613 %) at 375 nm(540 nm) weak light illumination under an external bias of -2V respectively.Clearly, reasonably good responses of the proposed photodetector are observed in both the UV and visible regions. The fabricated device not only exhibits fast response but also notable responsivity ,EQE and detectivity are also attained. The device photoresponse pattern under white light-ON/OFF,UV as well in Visible light with multiple (ON/OFF) cycles confirms the stable performance of the proposed device. The stable photoresponse and reasonably good performance by employing these ternary nanocomposites-based tetrapod shaped CdSe NCs into the binary PCDTBT:PCBM composite. This may consider to be one of the promising candidates for low-cost high-performance solution processed wideband photodetectors.

3.4 Conclusions

In this chapter, the nanocomposites of tetrapod shaped CdSe NCs and PCDTBT: PCBM blends have been explored for demonstrating a wideband UV-visible photodetector using ZnO nanorods as the ETL of the device. The fabricated device showed stable photoresponse characteristics under on/off modulation of UV, visible and broadband light in an open atmosphere. Under -2 V bias, the proposed device showed a responsivity of 1830 mAW^{-1}

(344 mAW^{-1}), detectivity of $1.75x10^{12}$ ($3.3x10^{11}$) Jones, reasonably fast rise time of 5.73 s (0.02 s) and fall time of 6.41s (0.14 s) at 375 nm (540 nm). Although the device fabrication has been carried out in a robust open environmental condition, the device showed a good response speed and high performance with good photoresponse behavior as well. We still believe that further improvement can be achieved in the device if fabricated under controlled environment. These ternary nanocomposites may consider to be one of the promising candidates for the development of the low-cost solution processed wideband hybrid photodetectors